

# A long look at the BALQSO LBQS 2212-1759 with XMM-Newton

J. Clavel,<sup>1</sup> N. Schartel<sup>2</sup> and L. Tomas<sup>2</sup>

<sup>1</sup> Research & Scientific Support Department, ESTEC, SCI-SA, Postbus 299 2200 AG - Noordwijk, The Netherlands  
e-mail: Jean.Clavel@esa.int

<sup>2</sup> XMM-Newton Science Operations Centre, ESAC, Apartado 50727, 28080, Madrid, Spain  
e-mail: nscharte@xmm.vilspa.esa.es, ltomas@xmm.vilspa.esa.es \*

Received: 7 September 2004 / Accepted: 9 September 2005

**Abstract.** Very long (172 ks effective exposure time) observations of the BALQSO LBQS 2212-1759 with *XMM-Newton* yield a stringent upper-limit on its 0.2–10 keV (rest-frame 0.64–32.2 keV) flux,  $F_{0.64-32.2} \leq 6 \times 10^{-17}$  erg cm<sup>-2</sup> s<sup>-1</sup>, while simultaneous UV and optical observations reveal a rather blue spectrum extending to 650 Å in the source rest frame. These results are used to set a tight upper-limit on its optical to X-ray spectral index  $\alpha_{\text{ox}} \leq -2.56$ . Given the HI-BAL nature of LBQS 2212-1759, its X-ray weakness is most likely due to intrinsic absorption. If this is the case, and assuming that the intrinsic  $\alpha_{\text{ox}}$  of LBQS 2212-1759 is  $-1.63$  – a value appropriate for a radio-quiet quasar of this luminosity – one can set a lower limit on the X-ray absorbing column  $N_{\text{H}} \geq 3.4 \cdot 10^{25}$  cm<sup>-2</sup>. Such a large column has a Thomson optical depth to electron scattering  $\tau_{\text{Th}} \geq 23$ , sufficient to extinguish the optical and UV emission. The problem only gets worse if the gas is neutral since the opacity in the Lyman continuum becomes extremely large,  $\tau_{\text{Ly}} \geq 2 \times 10^8$ , conflicting with the source detection below 912 Å. This apparent contradiction probably means that our lines-of-sight to the X-ray and to the UV emitting regions are different, such that the gas covers completely the compact X-ray source but only partially the more extended source of ultraviolet photons. An extended ( $\approx 1'$ ) X-ray source is detected  $\sim 2'$  to the south-east of the QSO. Given its thermal spectrum and temperature ( $1.5 \leq T \leq 3.0$  keV), it is probably a foreground ( $0.29 \leq z \leq 0.46$ ) cluster of galaxies.

**Key words.** quasars: absorption lines – quasars: individual – X-rays: individuals – Galaxies: active

## 1. Introduction

Broad Absorption Line (BAL) quasars are characterized by broad and blueshifted absorption troughs in their spectrum, from resonance transitions such as CIV $\lambda$ 1550, Ly $\alpha$  $\lambda$ 1216, NV $\lambda$ 1240, indicating the presence of a high velocity (up to 50,000 km s<sup>-1</sup>) outflow along the line-of-sight (LOS) to the nucleus. Taking into account selection biases, BALQSOs represent 22±4% of the radio-quiet quasar population (Hewett and Foltz 2003). The fraction of BALQSOs that are radio-loud is approximately the same as that of non-BAL quasars, but there appears to be a deficit of broad absorption line objects at large radio luminosities (Menou et al. 2001; Becker et al. 2000). Because of the overall similarity of their continuum and emission line properties with those of non-absorbed quasars, it is sometime thought that BALQSOs are “normal” quasars seen at a specific viewing angle such that our LOS intercepts a nuclear wind (Weyman et al. 1991). The wind possibly originates from the accretion disk and is driven out radially by radiation pressure (Murray et al. 1995). A hydrodynamic model for the

BAL wind was developed by Proga et al. (2000). In the empirical scenario proposed by Elvis (2000), the wind arises vertically from a narrow range of disk radii and bends outward to a cone angle of  $60^\circ$  with a divergence angle of  $6^\circ$ . In this type of models, it is the solid angle covered by the outflow that determines the fraction of BAL quasars. An alternative class of models speculates that the BAL phenomenon represents an early “cocoon” phase in the evolution of a QSO (e.g. Briggs, Turnshek and Wolfe 1984). Although his results are based on a small sample that contains only 4 BALQSOs, Boroson 2002 brought some credibility to this idea by showing that BALQSOs occupy a specific location in the quasar parameter space, characterized by large accretion rates and luminosities, close to the Eddington limit. The evolution scenario is also supported by the large fraction of BALQSOs found in a spectroscopic follow-up to the VLA FIRST survey – 29 radio-selected BALQSOs (Becker et al. 2000) – since the properties of the sample appear inconsistent with simple unified models.

BALQSOs are invariably X-ray weak or silent (Green et al. 1995; Green & Mathur 1996; Gallagher et al. 1999), suggesting the presence of very large absorbing columns,  $N_{\text{H}} \geq 10^{23}$  cm<sup>-2</sup>, 2-3 orders of magnitudes larger than those inferred from UV absorption line studies. This discrepancy led to the conclusion that the bulk of the absorbing gas is highly ionised and thus

Send offprint requests to: J. Clavel

\* This work is based on observations obtained with XMM-Newton, an ESA science mission with instruments and contributions directly funded by ESA Member States and the USA (NASA).

**Table 1.** Details of the XMM-Newton X-ray observations

Obs ID	Start Date	exposure times (s)	
		EPIC pn	EPIC MOS 1&2
0106660101	2000-11-17	55,718	2×57,824
0106660201	2000-11-18	50,618	2×52,724
0106660401	2001-11-18	0	2×33,050
0106660501	2001-11-17	8,208	2×10,822
0106660601	2001-11-17	106,808	2×109,422

mostly transparent in the ultraviolet while still providing large X-ray opacities. However, it was subsequently realized that the column densities derived from curve of growth analysis of absorption lines may be severely underestimated. High resolution and high signal-to-noise ratio UV spectra show that the lines are saturated despite the existence of residual flux at their bottom (e.g. Arav et al. 1999; Wang et al. 1999). The residual flux may be due to partial covering of the continuum source or to the scattering of part of its emission back into our LOS, as indicated by the higher degree of polarisation of BALQSOs as compared to non-BAL quasars (e.g. Schmidt and Hines 1999; Ogle et al. 1999).

Here we present very sensitive observations of the  $z = 2.217$  BALQSO LBQS 2212-1759 (Morris et al. 1991) performed with *XMM-Newton*. This quasar was selected because of its optical brightness ( $m_B = 17.94$ ) and tentative 3-sigma detection in the soft-X-ray band with ROSAT (Green et al. 1995). LBQS 2212-1759 displays two CIV $\lambda$ 1548 absorption troughs blue-shifted respectively by  $\simeq -6,300$  and  $-4,000$   $\text{kms}^{-1}$  with respect to its systemic velocity (Korista et al. 1993).

## 2. Observations and data reduction

LBQS 2212-1759 was observed twice with *XMM-Newton* (Jansen et al. 2001). The first observation took place from 22h15m (U.T.) on November 17, 2000 to 17h44m on November 18, under conditions of extremely low particle radiation background. The quasar was observed again one year later, from 22h17m on November 17, 2001 to 04h53m on November 19. On each occasion, data were collected simultaneously with all X-ray instruments on board *XMM-Newton*: the *EPIC-pn* (Strüder et al. 2001), the two *EPIC-MOS* (Turner et al. 2001), as well as the two *RGS* spectrographs (den Herder et al. 2001). As expected, the last did not yield any useful information and the corresponding data are not discussed further in the remainder of this paper. A log of the X-ray observations is provided in Table 1, where we give the *XMM-Newton* observation identifier in column 1, the start date of the observation in column 2 and the exposure times with the three *EPIC pn* and *EPIC MOS* instruments in column 3 & 4, respectively. Note the very long cumulative exposure time of the X-ray observations. In the case of the most sensitive *EPIC-pn* instrument, it reaches 221,352 s. Even after data screening the cumulative useful integration time of the *EPIC pn* data remains 172,628 s.

The X-ray *pn* and *MOS* data were reduced and analyzed in a standard fashion using the SAS v5.3. The pipe-line products of observation 0106660601 provide 44 positional coincidences between sources of the USNO-A2.0 Catalogue (Monet et al.

**Table 2.**  $3 - \sigma$  Upper limits to the X-ray flux of LBQS 2212-1759 derived from the EPIC-pn observations

energy band (keV)	Count rate ( $10^{-5} \text{ s}^{-1}$ )	Flux ( $10^{-16} \text{ erg cm}^{-2} \text{ s}^{-1}$ )
0.2–0.5	$\leq 9.03$	$\leq 1.69$
0.5–2.0	$\leq 9.25$	$\leq 2.74$
2.0–10.0	$\leq 8.65$	$\leq 14.2$
5.0–10.0	$\leq 6.16$	$\leq 20.1$
0.2–10.0	$\leq 1.48$	$\leq 0.64$

1998) and X-ray sources in the field of LBQS 2212-1759. Of these 44 coincidences, 35 X-ray sources have only one, three X-ray sources have two and one X-ray source has three optical counterparts. Restricting to the 35 X-ray sources with a unique optical identification, we infer a mean offset of  $2.2''$  between the X-ray position and the optical source coordinates. Note that out of these 35 X-ray sources with a unique identification, 25 (i.e. 63%) lie within  $2''$  of their optical counterpart. The BAL quasar was not detected in either of the X-ray instruments. The nearest detected X-ray point source is  $\sim 0.5'$  away from the nominal position of LBQS 2212-1759 (R.A. = 22:15:31.6; Dec. = 17:44:06 - J2000).

From the *r.m.s.* background count fluctuations in a  $9 \times 9$ -pixel cell centered on the expected source position, we computed  $3\sigma$  upper limits to the count rate in various energy bands. The HEW of the EPIC-pn point-spread function is  $14''$  and one CCD pixel projects onto an area of  $4.1 \times 4.1''$  on the sky. From the *XMM-Newton* observation of Q 0056-363, we determined the ratios between the total count rate of a faint point-source and the count rates measured in a  $9 \times 9$ -pixel cell centered on the source for each of the energy bands. These ratios were then applied to the cell upper limits to derive effective upper limits to the source count rate. The results are listed in table 2. These count rates were converted into flux upper limits using the *PIMMS* software available on-line at the HEASARC website. The results are given in Table 2 where we only list the results from the *EPIC pn* data, since the less sensitive *EPIC MOS* detectors yield consistent but significantly higher and therefore less constraining limits.

In an attempt to understand why LBQS 2212-1759 was marginally detected by Green et al. 1995, we checked their original ROSAT image. There are definitely no excess counts at the centre of their  $3'$  radius extraction circle, clearly ruling out the presence of a point-source. However, the merged EPIC data reveal the existence of a weak *extended* source, centered at R.A. = 22:15:37 and Dec = -17:45:35 and whose radius is  $1.0'$ . This source is most probably a foreground cluster of galaxies since its spectrum is well described by a Mekeal spectrum with temperature in the range 1.5–3 keV and a redshift between 0.29 and 0.46. Whatever its origin, this source clearly lies within the ROSAT extraction region and is likely the origin of the false detection of LBQS 2212-1759 by Green et al. 1995. The extended source was too weak to appear in the ROSAT All Sky Survey catalogue (1RXS) and could not therefore be taken into account by Green et al. 1995. Note that there are no EPIC point-

sources within the 10-20' annulus which these authors used to measure the background in the ROSAT image.

In parallel to the X-ray observations, a series of optical and ultraviolet broad-band filter images of the QSO field were obtained with the Optical Monitor telescope (*OM*; Mason et al. 2001) on board *XMM-Newton*. The *OM* data were reprocessed with the SAS version 6.0 using the script *omichain*. For each broad-band filter image, the corrected net count rate of the QSO was read-off directly from the SWSRLI output files, which lists all sources automatically detected by the SAS software, together with their count rate, statistical significance, measured coordinates, the associated errors and various data quality indicators. We used the close-by 13<sup>th</sup> magnitude star *S3211320188* from the HST guide-star catalog to correct for small ( $\leq 4''$ ) residual astrometric distortions in the *OM* coordinate system. After correction, the QSO coordinates as measured with *OM* agree to better than 1'' with *NED* catalog coordinates. The count rates were converted into fluxes following the recipe provided on the SAS web page at URL [xmm.vilspa.esa.es/sas/documentation/watchout/uvflux.html](http://xmm.vilspa.esa.es/sas/documentation/watchout/uvflux.html). The final fluxes are listed in Table 3, which provides: the observation identifier in column 1, the *OM* exposure number in column 2, the date and U.T. time of the start of the exposure expressed as a fractional day of 2000 in column 3, the filter identifier in column 4 and the flux with its associated statistical *r.m.s.* error in column 5. Early observations with the less sensitive UVW2 filter had exposure times that were too short and did not yield statistically significant detections. In such cases, 3 -  $\sigma$  upper limits are listed in Table 3.

A  $\chi^2$  test shows that the flux of LBQS 2212-1759 remained constant within the measurement uncertainties in all 6 filters. The reduced chi-squares (d.o.f.) corresponding to the hypothesis of a constant flux are  $\chi^2_{\nu} = 0.88$  (8), 0.53(9), 1.19 (9), 0.52 (10) and 1.20 (6) for the V, B, U, UVW1 and UVM2 filters, respectively. We therefore averaged the results from individual exposures and computed the weighted mean flux in each filter and the error on the mean. The near-IR *J*, *H* and *K* fluxes of LBQS 2212-1759 were retrieved from the 2MASS catalog (Kleinmann 1994; Barkhouse and Hall 2001). All fluxes were finally corrected for foreground galactic extinction ( $E_{b-v} = 0.026$ ; Schlegel et al. 1998; Cardelli et al. 1989). The results are given in Table 4, where we list the origin of the data in column 1, the effective wavelength and band-pass of the filter in the observer's frame in column 2 and column 3, respectively, the effective wavelength and band-pass of the filter in the quasar rest-frame in column 4 and column 5, respectively and the averaged de-reddened flux in column 6.

The rest-frame optical to EUV energy distribution of LBQS 2212-1759, is shown in Figure 1. A spectrum of LBQS 2212-1759 obtained by K. Korista in 1992 (Korista et al. 1993) and kindly provided to us by the author is also displayed for comparison. Note that while the flux increased by 46 % in the OM-V band during the 8.5 years interval between the two observations, the spectral shape remained very similar.

### 3. Implications and discussion

The UV-optical SED of LBQS 2212-1759 is typical of a high redshift QSO; at wavelengths longer than that of H-Ly $\alpha$ 1215, it displays a blue spectrum giving rise to an excess emission, the so-called "big blue bump", usually attributed to the thermal emission of an accretion disk. A power-law ( $F_{\nu} \propto \nu^{\alpha}$ ) fit to the 5 data-points with  $\lambda_{\text{rest}} \geq 1215 \text{ \AA}$  yields a spectral index  $\alpha = -0.96 \pm 0.18$ . Such an index is within the range of optical-UV slopes observed in the general quasar population. As noted by several authors (see e.g. Elvis et al. 1994), the spread in indices is fairly large. In the Francis et al. (1991) sample of 688 LBQS quasars for instance, indices vary from -1.5 to +1. The 1050–2200  $\text{\AA}$  spectral index of the average composite quasar of Zheng et al. (1997) is  $-0.86 \pm 0.01$ , while the mean 1285–5100  $\text{\AA}$  spectral index of the radio-quiet QSO sample of Kuhn et al. (2001) is  $-0.32 \pm 0.28$  ( $1-\sigma$ ) and independent of redshift. The composite quasar spectrum of Vanden Berk et al. (2001), obtained by averaging 2200 QSO spectra from the Sloan Digital Sky Survey, has a 1350–4230  $\text{\AA}$  index of -0.44. At wavelengths shorter than 1215  $\text{\AA}$ , the LBQS 2212-1759 spectrum steepens to a softer spectral index  $\alpha = -2.62 \pm 0.16$ . Again, such a steepening is not unusual amongst quasars and has been reported by several authors (e.g. Zheng et al. 1997; Kuhn et al. 2001; Vanden Berk et al. 2001). In a "normal" high redshift quasar, this sharp steepening of the spectrum in the EUV is due to the onset of many intervening Lyman series absorption systems along the line-of-sight, the so-called "Lyman alpha forest". In a BALQSO like LBQS 2212-1759, the steepening can also be attributed, at least partly, to resonance absorption within the BAL nuclear outflow.

The ultraviolet spectrum of LBQS 2212-1759 is however difficult to reconcile with the above stringent upper limits on its X-ray flux. The optical-to-X-ray spectral index of a quasar (Zamorani et al. 1981),  $\alpha_{\text{ox}}$ , is defined as the spectral index of an hypothetical power-law connecting its flux density at 2500  $\text{\AA}$  and 2.0 keV in the QSO rest-frame,  $\alpha_{\text{ox}} = 0.384 \log \frac{F_{2\text{keV}}}{F_{2500}}$ . In radio-quiet non-BAL quasars, it is observationally confined to a range  $-1.1 \geq \alpha_{\text{ox}} \geq -1.9$  with a weak dependence on the source luminosity (Vignali et al. 2003; Strateva et al. 2005). Using the same cosmological parameters as these authors, the monochromatic luminosity of LBQS 2212-1759 at 2500  $\text{\AA}$  (rest wavelength) is  $L_{2500} = 1.7 \cdot 10^{31} \text{ erg s}^{-1}$ , Hz $^{-1}$ , which, according to eq. 6 of Strateva et al., predicts  $\alpha_{\text{ox}} = -1.63 \pm 0.03$ . Assuming a canonical photon spectral index  $\Gamma = -1.9$  for the 0.2–10 keV spectrum of LBQS 2212-1759 (e.g. Laor et al. 1997), and using the X-ray flux upper limits of Table 2, one can infer an upper limit to the monochromatic flux density at a rest energy of 2 keV ( $E_{\text{obs}} = 0.621 \text{ keV}$ ),  $F_{\nu}(2\text{keV}) \leq 1.0 \cdot 10^{-8} \text{ mJy}$ . One can derive the flux at  $\lambda_{\text{rest}} = 2500 \text{ \AA}$  by interpolation between the de-reddened fluxes in the J and V bands. Combining the two yields  $\alpha_{\text{ox}} \leq -2.56$ , steeper by  $\sim 1$  dex than the index predicted for a radio-quiet quasar of the same luminosity as LBQS 2212-1759. This is illustrated in Figure 2, where we plot the overall Spectral Energy Distribution (SED) of LBQS 2212-1759. The upper limit to its 2 keV flux is 263 times lower than that predicted by extrapolation of its 2500  $\text{\AA}$  flux density with a power-law of index  $\alpha_{\text{ox}} = -1.63$ . Assuming that the dif-

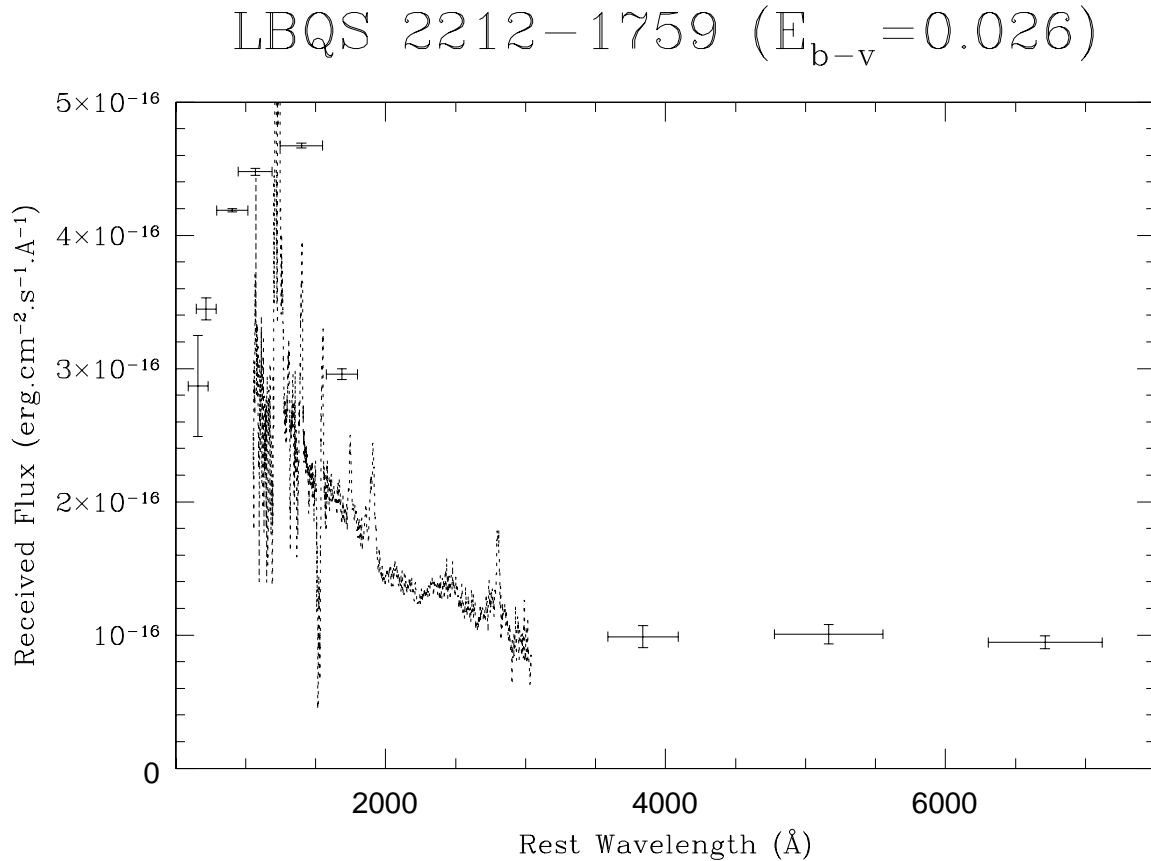


**Fig. 1.** The flux distribution of LBQS 2212-1759 from 6,711 Å to 659 Å (rest wavelengths). All data-points are from the present study, except for the 3 longest wavelengths ones which were retrieved from the 2MASS catalogue. The 1992 spectrum from Korista (1993) is also shown for comparison. All flux values are in the observer’s frame and have been corrected for foreground galactic extinction ( $E_{b-v} = 0.026$ ).

ference is entirely due to intrinsic absorption of the X-ray flux, one can infer a lower limit to the required absorbing column,  $N_H \geq 3.4 \cdot 10^{25} \text{ cm}^{-2}$ . Note that this result depends only weakly on the value assumed for the X-ray spectral index. For instance, using  $\Gamma = -2.5$  instead of  $-1.9$  hardly changes the results to  $N_H \geq 2.6 \cdot 10^{25} \text{ cm}^{-2}$ .

If the gas was neutral, an absorbing column as large as or larger than  $3.4 \cdot 10^{25} \text{ cm}^{-2}$  would create an optical depth at the Hydrogen Lyman limit,  $\tau_{Ly} \geq 2.2 \cdot 10^8$ , more than sufficient to extinguish all radiation at wavelengths shorter than 912 Å. This is not the case however, since LBQS 2212-1759 is detected to

$\lambda_{rest} = 659 \text{ Å}$ . Hence, the X-ray absorbing gas cannot be neutral and cover the UV continuum source. However, even if the gas is fully ionised, the Thomson optical depth to electron scattering corresponding to the above column,  $\tau_{th} \geq 23$ , is sufficient to attenuate the flux by a factor  $\approx 10^{10}$  and make LBQS 2212-1759 invisible at all wavelengths except in the  $\gamma$  ray regime. Another difficulty is that, unless the gas is completely free of dust, extinction will wipe-out any emerging UV and optical photon. Even if the dust to gas ratio is 100 times lower than the average galactic value (e.g. Gorenstein 1975), an absorbing column of  $3.4 \cdot 10^{25} \text{ cm}^{-2}$  would still generate  $\sim 150$  magnitudes

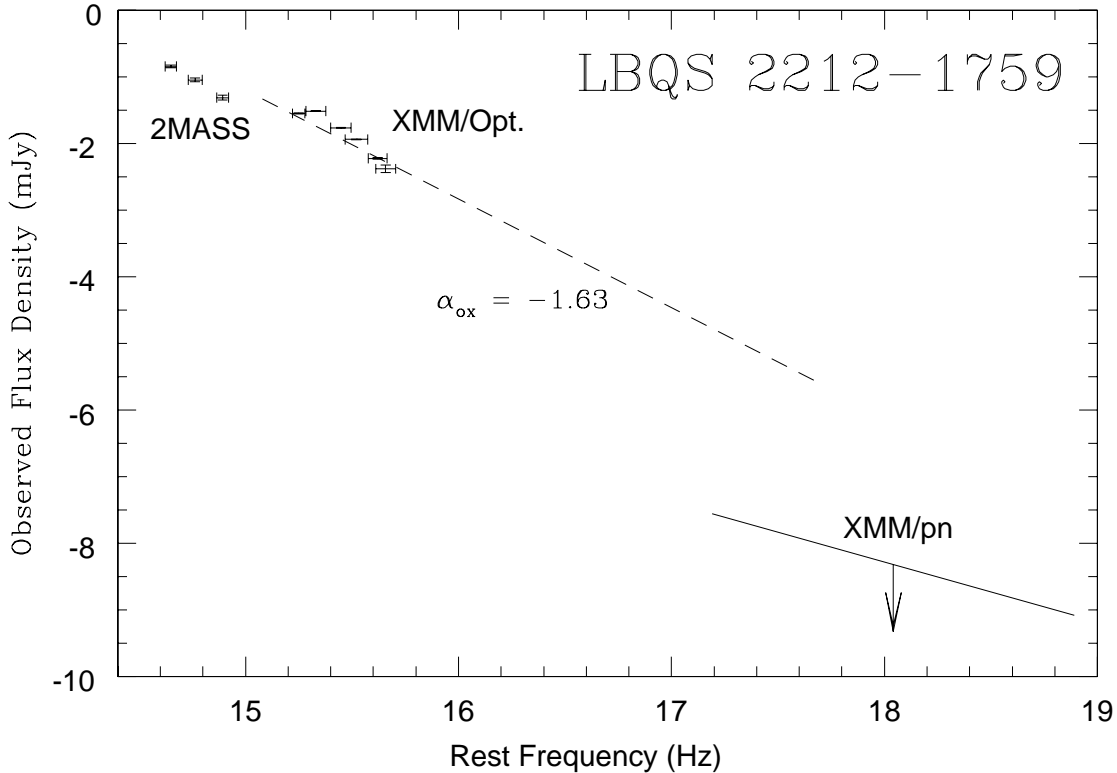


**Fig. 2.** The overall optical-to-X-ray spectral energy distribution of LBQS 2212-1759. All flux values are in the observer’s frame and have been corrected for foreground galactic extinction ( $E_{b-v} = 0.026$ ). The upper limit to the 0.2–10 keV (observer’s frame) flux of table 2 is shown as a spectrum of photon index  $\Gamma = -1.9$ . For comparison, a fiducial power-law of index  $\alpha_{ox} = -1.63$  and extending from 2500 Å to 2 keV (rest frame) is shown as a dashed line. The LBQS 2212-1759 flux upper limit is 263 times lower than the flux predicted by extrapolating the  $\alpha_{ox}$  power-law to 2 keV

of visual extinction and approximately ten times more in the far ultraviolet.

We are thus left with an inconsistency: on the one hand, LBQS 2212-1759 is detected with high statistical significance in the UV and EUV range, and on the other it is not detected in the X-rays, with upper limits on the 0.2–10 keV flux which, taken at face value, imply column densities sufficient to extinguish its ultraviolet emission as well.

In what follows, we briefly explore two possible explanations for this apparent contradiction:

1. *LBQS 2212-1759 is genuinely X-ray weak, with an intrinsic optical to X-ray spectral index  $\alpha_{ox} \leq -2.56$ :* available data, however, do not seem to support this hypothesis since the majority of BALQSO’s, once corrected for absorption, have a normal energy distribution. For instance, the 8 BALQSOs observed by Gallagher et al. (2002) with Chandra have a mean optical to X-ray spectral index  $\langle \alpha_{ox} \rangle = -1.58$ , with an *r.m.s.* dispersion of 0.11. Similarly, the 6 HI-BAL quasars detected by Green et al. (2001) also with Chandra have a mean index  $\langle \alpha_{ox} \rangle = -1.58$ , with an *r.m.s.* disper-

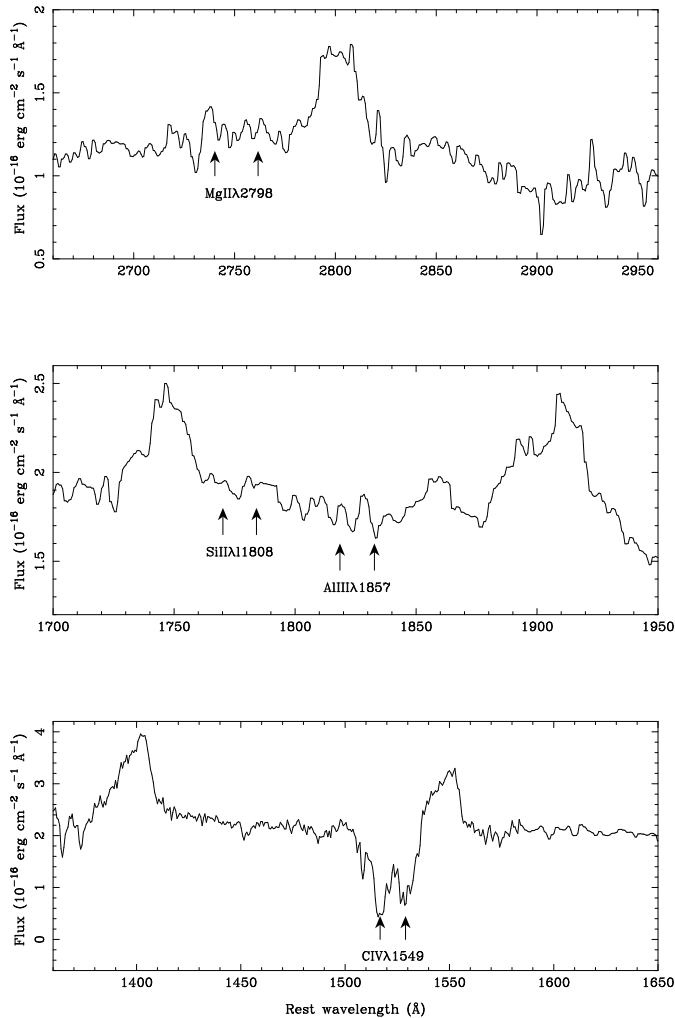


**Fig. 3.** The spectrum of LBQS 2212-1759 around the MgII $\lambda$ 2798 line (upper panel), the AlIII $\lambda$ 1857 and SiIII $\lambda$ 1808 lines (middle), and the CIV $\lambda$ 1549 line (bottom). The wavelengths at which one expects blue-shifted double absorption troughs are indicated with arrows. Note the absence of significant absorption from MgII, SiII and AlIII.

sion of 0.11. Two additional HI-BAL QSO’s observed with XMM-Newton by Grupe et al. (2003) have intrinsic values of  $\alpha_{\text{ox}}$  of -1.50 and -1.48, respectively. All these indices are entirely compatible with the value expected for radio-quiet non-BAL QSOs and much flatter than the upper limit in LBQS 2212-1759,  $\alpha_{\text{ox}} \leq -2.56$ . We note that the two LO-BAL quasars detected by Green et al. (2001), IRAS 07598+6508 and FIRST J0840+3633 have *apparent* steep indices of -2.34 and -2.11, respectively, because they likely suffer from additional absorption which cannot be corrected for given the low signal-to-noise ratio of their X-ray spectra. We note that LBQS 2212-1759 is definitely not a LO-BAL since its spectrum lacks characteristic absorption lines from low ionisation species, such as SiII $\lambda$ 1808, AlIII $\lambda$ 1854 and MgII $\lambda$ 2798 (see Figure 3). Only two BALQSO’s seem to be genuinely X-ray deficient: with  $\alpha_{\text{ox}} = -1.96$ , PHL 1811 remains marginally X-ray weak after correction for internal absorption, though

**Table 5.** Intensities and full width at half maximum (FWHM) of the main emission lines in the spectrum of LBQS 2212-1759; all intensities are in units of  $10^{-16} \text{ erg cm}^{-2} \text{ s}^{-1}$  and have been corrected for galactic extinction. Their uncertainties are typically 10 %. The FWHM are expressed in  $\text{km s}^{-1}$  and have an uncertainty of  $\pm 50 \text{ km s}^{-1}$

Line ID	Flux	FWHM
H-Ly $\alpha$ $\lambda$ 1216	204	1610
NV $\lambda$ 1240	132	4780
SiIV $\lambda$ 1397	50	3600
CIV $\lambda$ 1549	33	2790
HeII $\lambda$ 1640	$\leq 4$	–
NIII] $\lambda$ 1750	25	2780
CIII] $\lambda$ 1909	49	5150
MgII $\lambda$ 2798	41	2590

this conclusion is not very robust given the paucity of X-ray photons detected (183; Leighly et al. 2001); the second BALQSO is PG 1254+047 for which Sabra and Hamann (2001) present convincing evidence that it is at the same time intrinsically X-ray weak ( $\alpha_{\text{ox}} \leq -2.0$ ) and heavily absorbed ( $N_{\text{H}} = 2.8 \times 10^{23} \text{ cm}^2$ ). We note that the indices of both sources are still significantly larger than the upper limit on  $\alpha_{\text{ox}}$  of LBQS 2212-1759. One can in principle gauge the slope of the optical-to-X-ray spectrum of LBQS 2212-1759 from its relative emission line intensities. Indeed, if the QSO was lacking EUV and soft X-rays, one would expect the high ionisation emission lines to be relatively weak compared to lines from lower ionisation species. In Table 5, we list the (de-reddened) intensities of the main emission lines together with their Full-Width at Half-Maximum (FWHM). The HeII $\lambda$ 1640 line is undetected, which, at first sight, could be indicative of a deficiency in EUV and soft X-rays. We note however, that the upper limit on its intensity relative to that of e.g. CIV $\lambda$ 1249, 0.12, is still higher than that in the average composite SDSS spectrum of Vanden Berk et al. (2001), 0.02, and therefore not particularly useful. Furthermore, the NV $\lambda$ 1240 line is quite strong, with an intensity relative to Ly $\alpha$  $\lambda$ 1216, NV/Ly $\alpha \approx 0.65$ , compared to e.g. 0.025 in the average composite SDSS spectrum. Since the photon energy required to ionize N $^{3+}$  into N $^{4+}$  is 77.5 eV, much larger than the He $^{+}$  ionisation potential, 24.6 eV, a deficit of EUV and soft X-ray photons seems implausible. In fact, the NIII]  $\lambda$ 1750 is also quite strong (see also Fig. 3), with an intensity relative to Ly $\alpha$  $\lambda$ 1216, III]/Ly $\alpha \approx 0.12$ , 32 times larger than that in the average composite SDSS QSO spectrum (Vandeb Berk et al. 2001). This suggests an overabundance of Nitrogen in LBQS 2212-1759. The CIII]  $\lambda$ 1909/CIV $\lambda$ 1549 intensity ratio, 1.49, is 2.3 times larger than that of the composite SDSS QSO (0.63), but this is partly due to absorption eating away a fraction of the blue wing of the CIV emission line. In summary, the emission line intensity ratios do not provide conclusive evidence for a deficit in EUV and soft X-rays in LBQS 2212-1759.

2. *The LOS to the optical-UV source is different from that to the X-ray source:* with a “balnicity index” (Weyman et al.

1991) of  $2221 \text{ km s}^{-1}$  (Korista et al. 1993), LBQS 2212-1759 exhibits relatively weak BAL. Moreover, only about 80 % of its continuum flux is absorbed at the bottom of the CIV $\lambda$ 1550 trough, indicating partial coverage of the UV source (Korista et al. 1993). Similarly, model-fits of the X-ray spectrum of the few BALQSOs detected at high energies also tend to require partial covering of the X-ray source (though models with an ionized absorber yield equally acceptable fits). In lower luminosity AGNs, different variability timescales in the two wavebands clearly demonstrate that the X-ray source is  $\sim$  an order of magnitude more compact than the UV-optical source. It thus remains a possibility that, in some BALQSOs at least, the outflow intercepts only a fraction of the UV-optical emission while completely blocking-out the X-ray flux. Gallagher et al. (2004) reach a similar conclusion for the BALQSO PG 2112+059 based on dramatically different patterns of variability in the X-ray and the UV regime. In PG 2112+059 as well, the absence of a Lyman edge sets an upper limit to the UV continuum absorbing column  $N_{\text{H}} \leq 10^{17} \text{ cm}^{-2}$ , 5–6 orders of magnitude lower than the absorbing column covering the X-ray source.

In the absence of a better choice, hypothesis number two remains our favorite explanation for the peculiar SED of LBQS 2212-1759, though we cannot rule-out the alternative possibility that LBQS 2212-1759 is genuinely X-ray weak, with an intrinsically steep index,  $\alpha_{\text{ox}} \leq -2.56$ . Obviously more observations with *Chandra* and *XMM-Newton* are required to increase the number of BALQSOs with measured X-ray properties or at least with stringent upper limits.

*Acknowledgements.* The authors are grateful to Kirk Korista for providing his 1991 optical spectrum of LBQS 2212-1759 in electronic form. The anonymous referee is also thanked for constructive comments which significantly improved this article.

This publication makes use of data products from the Two Micron All Sky Survey, which is a joint project of the University of Massachusetts and the Infrared Processing and Analysis Center/California Institute of Technology, funded by the National Aeronautics and Space Administration and the National Science Foundation.

This research has made use of the *NASA/IPAC Extragalactic Database (NED)* which is operated by the Jet Propulsion Laboratory, California Institute of Technology, under contract with the National Aeronautics and Space Administration.

## References

- Arav, N. et al. 1999, ApJ516, 27  
 Barkhouse, W.A. & Hall, P.B. 2001, AJ121, 2843  
 Becker H.R. et al. 2000, ApJ538, 72  
 Boroson, T.A. 2002, ApJ565, 78  
 Briggs F.H., Turnshek, D.A. & Wolfe, A.M. 1984, ApJ287, 549  
 Cardelli, J.A., Clayton, G.C., Mathis, J.S. 1989, ApJ345, 245  
 den Herder, J.W. et al. 2001, A&A365, L7  
 Elvis, M. et al. 1994, ApJS95, 1  
 Elvis, M. 2000, ApJ545, 63  
 Francis, P.J. et al. 1991, ApJ373, 465.  
 Gallagher, S.C. et al. 1999, ApJ519, 549  
 Gallagher, S.C. et al. 2002, ApJ567, 37  
 Gallagher, S.C. et al. 2004, ApJ603, 425  
 Gorenstein, P. 1975, ApJ198, 95  
 Green, P.J. et al. 1995, ApJ450, 51  
 Green, P.J. & Mathur S. et al. 1996, ApJ462, 637  
 Green, P.J. et al. 2001, ApJ558, 109  
 Grupe, D., Mathur, S. & Elvis, M. 2003, AJ126, 1159  
 Haardt, F. & Maraschi, L. 1991, ApJ380, L51  
 Hewett, P.C. & Foltz, C.B. 2003, AJ125, 1784  
 Jansen, F. et al. 2001, A&A365, L1  
 Kleinmann, S.G. et al. 1994, Ap&SS217, 11.  
 Korista, K.T. et al. 1993, ApJS88,357  
 Kuhn, O. et al. 2001, ApJS136, 225  
 Laor, A. et al. 1997, ApJ477, 93  
 Leighly, K.M. et al. 2001, AJ121, 2889  
 Mason et al. 2001, A&A365, L36  
 Menou, K. et al. 2001, ApJ561, 645  
 Monet, D. et al. 1998, USNO-A V2.0, A Catalog of Astrometric Standards U.S. Naval Observatory Flagstaff Station (USNOFS) and Universities Space Research Association (USRA) stationed at USNOFS.  
 Morris, S.L. et al. 1991, AJ102, 1627  
 Murray, N. et al. 1995, ApJ451, 498  
 Ogle, P.M. et al. 1999, ApJS125, 1  
 Proga, D. et al. 2000, ApJ543, 686  
 Sabra, B.M. & Hamann, F. 2001, ApJ563, 555  
 Schmidt, G.D. & Hines, D.C. 1999, ApJ512, 125  
 Schlegel, D.J., Finkbeiner, D.P.; Davis, M. 1998, ApJ500, 525  
 Strateva, I.V. et al. 2005, AJ130, 387  
 Strüder, L. et al. 2001, A&A365, L18  
 Turner, M.J.L. et al. 2001, A&A365, L27  
 Vanden Berk, D.E. et al. 2001, AJ122, 549  
 Vignali, C., Brandt, W.N., and Schneider, D.P. 2003, AJ125, 433  
 Wang, T.G. et al. 1999, ApJ519, L35  
 Weyman, R.J. et al. 1991, ApJ373, 23  
 Zamorani, G. et al. 1981, ApJ245, 357  
 Zheng, W. et al. 1997, ApJ475, 469

**Table 3.** Optical & UV fluxes measured through the various OM filters

Obs ID	Exposure #	Start date (2000 day #)	Filter	Flux ( $10^{-16}$ erg cm $^{-2}$ s $^{-1}$ Å $^{-1}$ )
106660101	10	321.78944	V	2.79 ± 0.33
106660101	401	321.80242	V	3.32 ± 0.33
106660101	402	321.81542	V	2.72 ± 0.33
106660101	403	321.82841	V	2.80 ± 0.32
106660101	404	321.84140	V	3.00 ± 0.33
106660201	6	322.54738	V	2.77 ± 0.30
106660201	401	322.56269	V	2.42 ± 0.30
106660201	402	322.57797	V	2.41 ± 0.30
106660201	403	322.59329	V	2.47 ± 0.29
106660101	8	321.91927	B	4.33 ± 0.22
106660101	409	321.93226	B	4.36 ± 0.22
106660101	410	321.94523	B	4.42 ± 0.22
106660101	411	321.95822	B	4.25 ± 0.21
106660101	412	321.97122	B	3.95 ± 0.22
106660201	9	322.70034	B	4.23 ± 0.20
106660201	409	322.71564	B	4.17 ± 0.20
106660201	410	322.73094	B	4.12 ± 0.20
106660201	411	322.74624	B	4.35 ± 0.20
106660201	412	322.76154	B	4.02 ± 0.20
106660101	7	321.85435	U	3.84 ± 0.20
106660101	405	321.86733	U	4.13 ± 0.20
106660101	406	321.88032	U	4.12 ± 0.20
106660101	407	321.89332	U	4.11 ± 0.20
106660101	408	321.90630	U	3.59 ± 0.20
106660201	8	322.62387	U	4.00 ± 0.18
106660201	405	322.63916	U	3.83 ± 0.18
106660201	406	322.65446	U	3.84 ± 0.18
106660201	407	322.66976	U	4.24 ± 0.18
106660201	408	322.68506	U	3.73 ± 0.18
106660101	9	321.98869	UVW1	3.85 ± 0.20
106660101	413	322.01070	UVW1	3.70 ± 0.20
106660101	414	322.05354	UVW1	3.60 ± 0.20
106660101	415	322.07557	UVW1	3.57 ± 0.19
106660101	416	322.09757	UVW1	3.73 ± 0.20
106660201	10	322.78260	UVW1	3.65 ± 0.18
106660201	413	322.80948	UVW1	3.68 ± 0.18
106660201	414	322.83636	UVW1	3.59 ± 0.18
106660201	415	322.86323	UVW1	3.60 ± 0.18
106660201	416	322.89011	UVW1	3.68 ± 0.18
106660501	6	686.10035	UVW1	3.39 ± 0.17
106660601	11	687.44819	UVW1	3.48 ± 0.11
106660101	10	322.11957	UVM2	3.28 ± 0.39
106660101	418	322.16359	UVM2	2.78 ± 0.39
106660101	419	322.18561	UVM2	2.97 ± 0.39
106660101	420	322.20762	UVM2	2.99 ± 0.39
106660401	9	685.93929	UVM2	2.41 ± 0.26
106660601	13	687.65182	UVM2	2.50 ± 0.24
106660101	11	322.23667	UVW2	< 6.60
106660101	422	322.30894	UVW2	< 7.19
106660101	423	322.34508	UVW2	< 6.56
106660101	424	322.38120	UVW2	3.48 ± 0.70
106660401	10	686.02503	UVW2	1.33 ± 0.58
106660501	8	686.15948	UVW2	< 8.16
106660601	14	687.74334	UVW2	2.20 ± 0.58
106660601	15	687.83490	UVW2	2.15 ± 0.58

**Table 4.** The flux of LBQS 2212-1759 as a function of wavelength, from the near-IR to the EUV. The values in the optical & UV have been obtained by averaging fluxes from individual OM exposures. All fluxes have been corrected for foreground galactic reddening

Instrument	$\lambda_{\text{obs}}$	$\Delta\lambda_{\text{obs}}$ ( $\text{\AA}$ )	$\lambda_{\text{rest}}$	$\Delta\lambda_{\text{rest}}$	Flux ( $10^{-16} \text{ erg cm}^{-2} \text{ s}^{-1} \text{ \AA}^{-1}$ )
2MASS K	21,590	2,620	6,711	814	$0.945 \pm 0.047$
2MASS H	16,620	2,510	5,166	780	$1.006 \pm 0.071$
2MASS J	12,350	1,620	3,839	504	$0.987 \pm 0.082$
OM-V	5,430	710	1,688	221	$2.957 \pm 0.040$
OM-B	4,500	980	1,399	305	$4.673 \pm 0.018$
OM-U	3,440	780	1,069	242	$4.478 \pm 0.026$
OM-UVW1	2,910	710	905	221	$4.186 \pm 0.013$
OM-UVM2	2,310	460	718	143	$3.447 \pm 0.082$
OM-UVW2	2,120	460	659	143	$2.868 \pm 0.379$